Heliyon 7 (2021) e07928

Contents lists available at ScienceDirect

Heliyon

journal homepage: www.cell.com/heliyon

Research article

Study of a printed split-ring monopole for dual-spectrum communications

Bright Yeboah-Akowuah [a], Eric Tutu Tchao [a], Masood Ur-Rehman [b], Mohammad Monirujjaman Khan [c,*], Sarosh Ahmad [d]

[a] Kwame Nkrumah Universtiy of Science and Technology, Department of Computer Science, Kumasi, Ghana
[b] Electronic Engineering, School of Engineering, University of Glasgow, James Watt Building, University Avenue, Glasgow, G12 8QQ, UK
[c] Department of Electrical and Computer Engineering, North South University, Bashundhara, Dhaka, 1229, Bangladesh
[d] Department of Electrical Engineering and Technology, Government College University Faisalabad, Pakistan

ARTICLE INFO

Keywords:
Dual-band
Industrial, scientific and medical (ISM)
Ultrawideband (UWB)
Planar monopoles

ABSTRACT

In this study, we present a low-profile dual-spectrum split-ring monopole that operates at industrial, scientific and medical (ISM) (2.45 GHz) band and ultrawideband (UWB) spectrum (3.1–10.6 GHz). We optimised the design for dual-band operations by using circular split-ring radiators. The coupling between both rings drives the structure to achieve quasi-resonance frequencies in the UWB spectrum. A small stub combines the two radiators and both behave as a single element that enables the antenna to resonate at ISM band 2.45 GHz. The antenna achieves the desired characteristics in terms of good impedance matching, radiation properties as well as other physical and practical requirements such as compact geometry, planar profile and easy fabrication. The very good agreement between the simulated and measured results show that the proposed antenna has the potential for dual-band application.

1. Introduction

Significant progress in the design of compact antennas with broadband, dual-frequency, and gain-enhanced operations have been achieved over the past several years. Most of the antennas that have been reported in the literature for dual-band and broadband operations have been for conventional narrow operating bandwidths [1, 2, 3, 4, 5]. A narrow bandwidth is a major disadvantage for practical applications. Moreover, modern-day communication systems require large bandwidth for high data transmission and resolution.

Although a lot of research works have been done on monopoles and split ring resonators, those techniques have been used for different applications and technologies. Monopole antennas have been used extensively for both narrow and ultra-wideband applications. Split ring resonators have been used for narrowband and multiband. However, little work has been carried out in order to realise the full potentials of integrating split ring resonators with planar monopole antennas (PMA) for dual-band communications. Previous works have not comprehensively addressed this issue but separate structures to cover different spectrum. Many systems operate in two or more frequency bands that require dual or triple band operations of fundamentally narrow band antennas. In some instances separate antenna elements were designed to operate in the frequency bands [6, 7, 8]. It is desirable and important to design antennas of single elements that have large bandwidth and cover excess frequency bands and various applications for modern communications.

Following Federal Communications Commission (FCC) licensing of UWB spectrum, the technology has gained momentum and attention from both academia and industry for research in short-range wireless communications and other applications [9]. The advantages of UWB over narrowband antennas include large bandwidth, high data rate, resistance to interference, and low power consumption. In addition to UWB spectrum is another important license-free frequency in the Industrial, Scientific and Medical (ISM) covering IEEE 802.11b and IEEE 802.11g band of 2.40–2.484 GHz [10].

In order to satisfy the aforementioned technologies, many planar monopole antennas (PMA) have been proposed and designed for some applications covering these frequency bands [11, 12, 13, 14, 15, 16, 17, 18, 19, 20]. These antennas employ complex geometries such as elliptical, modified circular, modified elliptical and many more. However, few of them consider the antennas to incorporate both ISM and UWB bands in a single element. Moreover, simple geometry is also a preferred choice to reduce complexity and inherent cost. Furthermore, to incorporate these bands in a single device, it is important to have a single

* Corresponding author.
E-mail address: monirujjaman.khan@northsouth.edu (M.M. Khan).

https://doi.org/10.1016/j.heliyon.2021.e07928
Received 12 July 2021; Received in revised form 30 July 2021; Accepted 1 September 2021

dual-band antenna to cover these bands. In this study, we propose a low profile and dual-band antenna to cover both ISM and UWB bands. The rest of the paper is structured as follows: Section 2 presents our antenna design and geometry, while Section 3 gives the results and discussions of the antenna performance, comparing simulated and measured results. Conclusions are given in Section 4.

2. Antenna geometry and design

The geometry of the proposed antenna consists of an *Ls Ws* = 40 × 30 mm^2 FR4 substrate of thickness 1.5 mm (with $\varepsilon_r = 4.7$, $\tan\delta = 0.01$). On top of the substrate is a radiator of a pair of split rings (SR) with aperture on the same side. The split rings are connected by a small stub. A thin slot is etched between the radiators to enhance coupling in the structure. At the back of the substrate is a partial rectangular ground plane measuring *gr Ws* mm^2. A 50Ω coaxial transmission line is used to feed the antenna. In de-signing the proposed monopole antenna, the lower band-edge frequency was estimated using the standard formulation given for cylindrical monopole antenna with suitable modification, Eq. (1) [21]. The UWB lower edge frequency (LEF) was estimated to fall in the lower UWB range (3.1–4.5 GHz) and the second resonance in the upper UWB (5.8–10.6 GHz) The optimised values have been shown in Table 1.

$$f = \frac{7.2}{L + r + p} \tag{1}$$

where *L* is the height of the planar monopole antenna in cm, r equivalent cylindrical monopole in cm, and p is the length of the feed line in cm.

With slight modification, here is more appropriate equation for the lower band-edge frequency given as:

$$f = \frac{7.2\sqrt{\varepsilon}}{L + r + p} \tag{2}$$

where the effective cylindrical monopole of the design is given as $r = 2\pi L$. The modified Eq. (2) with the dielectric material increases the effective dimensions of the monopole leading to reduction in the lower band-edge frequency which is estimated to be 3.4 GHz. This is confirmed by simulation studies where LEF was found to be 3.4 GHz.

One of the fundamental material properties is permittivity ε. Referring to Eq. (1), in a dielectric medium the wavelength λ is given as Eq. (3):

$$\lambda = \frac{c}{f\sqrt{\varepsilon}} \tag{3}$$

Theoretically, it is observed that if the wavelength λ of electromagnetic wave is reduced it affects the frequency of operation in a given medium. For the proposed antenna, in order to lower the frequency to ISM 2.45 GHz, the path of surface current distributions as shown in Figure 6 became longer which slows down the speed of light and eventually affecting the frequency of operation. The technique of making the current path longer in order to lower the operation frequency and miniaturisations have been employed in many applications [22, 23, 24, 25, 26].

Table 1. Optimised parameters of the proposed dual-spectrum antenna shown in Figure 1.

Parameter	Description	Value
Ls	substrate length	40 mm
W s	substrate width	30 mm
s	size of the aperture	0.4 mm
cg	coupling gap	1 mm
stub	length of the stub	7.4mm
*r*1	radius of inner ring	5 mm
*r*2	radius of outer ring	10 mm
*w*1	width of inner ring	2.6 mm
*w*2	width of outer ring	4 mm
gr	ground length	20 mm
wf	width of the microstrip line	2.6 mm

2.1. Parametric studies

In order to gain further insight into the performance of the proposed antenna with respect to indicators such as return loss, impedance matching, and gain, we studied the effects of key parameters, namely, the aperture *s*, coupling gap *cg*, and the *stub* with reference to Figure 1.

1) *Effect of the aperture (s):* In the design process we considered using aperture on the rings to tune the antenna to ISM band at 2.45 GHz and also rejection of 7.1–8 GHz band. We investigated four cases and followed the process shown in Figure 2.

Case 1: We designed the rings without any aperture. In this topology, we have two circular-ring radiators with coupling gap in-between, and fed by a 50Ω coaxial transmission line. By using circular ring radiators, wider bandwidths have been reported in the literature [2728]. The central part of the radiator has been cut, since most of the currents travel along the edges. With reference to Figure 3, it is observed that the antenna covers a portion of upper UWB spectrum and completely outside the required ISM 2.45 GHz frequency.

Case 2: In case 2, we examined possible cases of where to place the aperture on the rings. We etched the aperture on the outer ring alone to examined its effect, therefore, a slit is cut on the outer ring to break the current path along the edges. A slit on the outer ring (Refer to Figure 2) improves the bandwidth in the UWB spectrum as shown in S_{11} response in Figure 3, however, it was still outside the ISM 2.45 GHz band as desired in this study.

Case 3: We also considered the aperture on the inner ring alone. Just like Case 2, we observed the effect of the slit on the inner ring. The S_{11} response in Figure 3 shows that the aperture on the inner ring changes the impedance matching especially at 3.5 GHz where the signal was spurious.

Case 4: In this case, we cut slit on both rings and aligned them in the same direction. The slits on both rings improve the impedance matching slightly as compared to the other cases (Refer to Figure 3). The four cases considered show that the slit *s* has an impact on the impedance matching and bandwidth.

2) *Effects of the coupling gap (cg):* The impact of the gap between the split-ring radiators (SRR) was investigated. We assess the effects in terms of the impedance matching and bandwidth of operation. Figure 4 shows the simulated return loss performance of different values of coupling gap (cg = 1, .2,3, 4). It can be inferred from the results that the

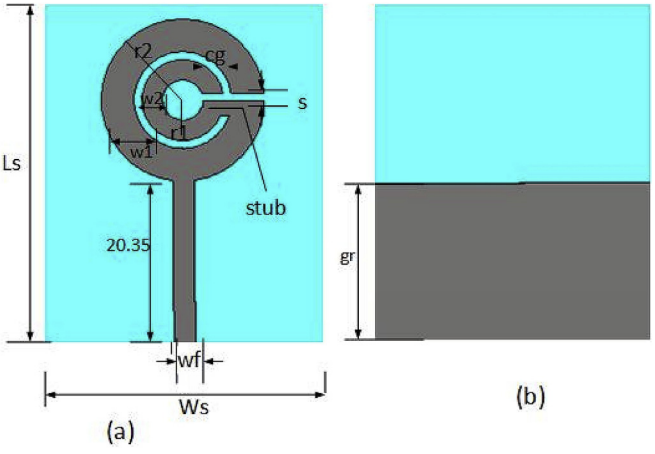

Figure 1. Geometry and dimensions of the proposed dual-spectrum antenna (all units are in mm): (a) top view (b) bottom view.

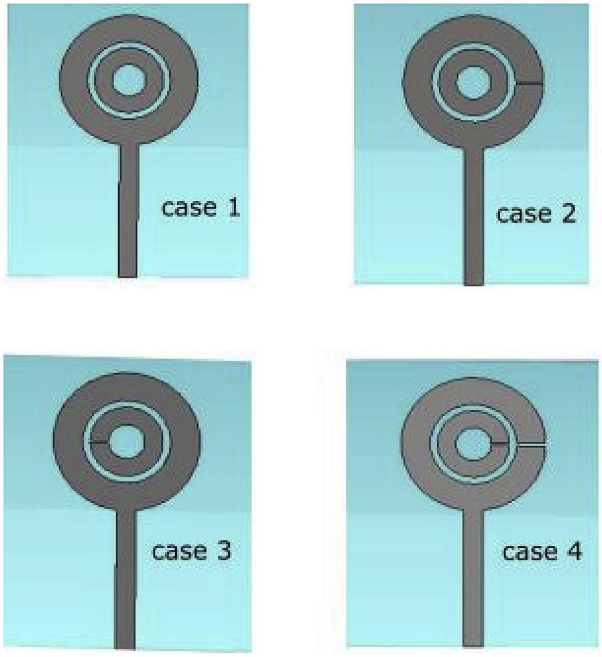

Figure 2. Topology and design process of the proposed dual-spectrum antenna. Figure panels: (case 1) rings without aperture, (case 2) aperture on outer ring only, (case 3) aperture on inner ring only, and (case 4) aperture on both inner and outer rings.

optimal coupling gap cg = 1 offers the best impedance matching at frequency 2.45 GHz.

3) *Effect of the stub:* The results from our study indicate that without the stub connecting the SRRs, the proposed structure operates in UWB spectrum However, with the stub connecting the SRRs, the current paths along the rings become longer and support the antenna to operate in the ISM band 2.45 GHz as shown in Figure 5. It is also noted that the stub improves the impedance matching and enhance the bandwidth.

2.2. Operating principles

Split-ring resonators (SRR) have been employed for multi-band antennas for multiple applications. In essence, simple printed monopoles or dipoles have been loaded with slots to produce resonance frequencies

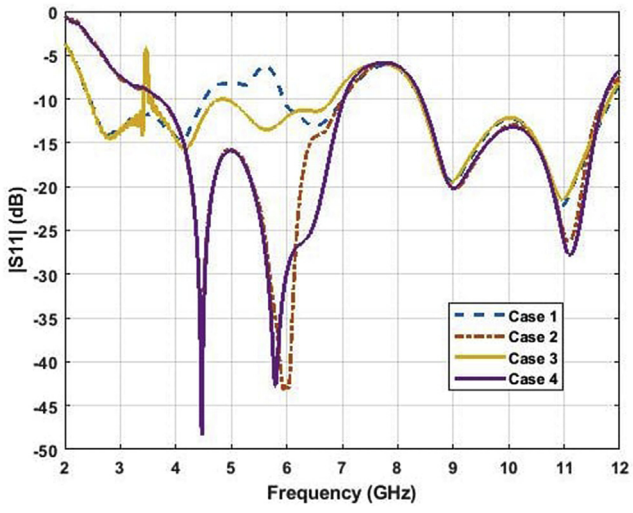

Figure 3. Effects of the aperture *s* on the performance of the proposed dual-spectrum antenna.

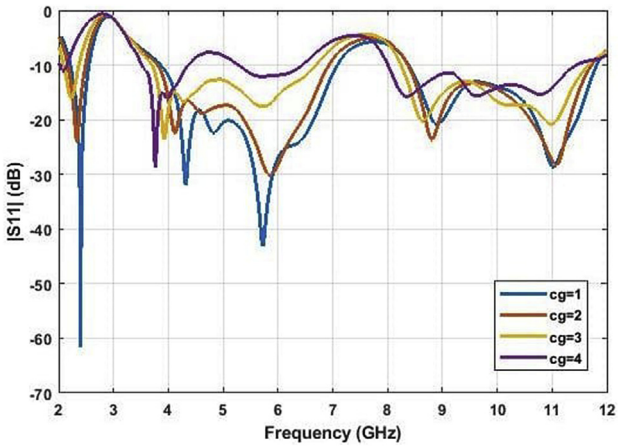

Figure 4. Effects of the coupling gap *cg* between the split-ring radiators.

[29, 30, 31, 32, 33]. In most cases, the slots are inserted at strategic points where the current flow is less predominant. With this approach, the printed monopoles keep their basic benefits and properties while dual or multiband modes are achieved with design techniques.

To illustrate our approach, we employ two circular-ring radiators with apertures. The two circular-rings are joined together with a stub which enables both to act as a single element. We take advantage by optimising the coupling between both rings that enable the structure to behave as an effective medium to support quasi-resonance frequencies in the ultra-wideband spectrum. The quasi-resonant phenomenon is driven by an axial time-varying electric fields. With the rings becoming a single element by virtue of the stub connecting them and coupled aperture, the long current path along the periphery of the rings drives the first resonance frequency to a low value of 2.45 GHz. Furthermore, the aperture *s* cut from the radiator causes perturbation of surface current distribution. The aperture introduces series inductance and capacitance resulting in strong interaction between the radiator and the notch and the effect is rejection of some bands 7.1–8 GHz.

The partial ground plane and the microstrip feed line provide stable transmission and balancing to the structure. A standing wave pattern can also be observed from the surface current distribution as evidence at the selected frequencies as shown in Figure 6.

3. Results and discussions

The prototype of the proposed dual-spectrum antenna with the optimised values presented in Table 1 was fabricated. The prototype,

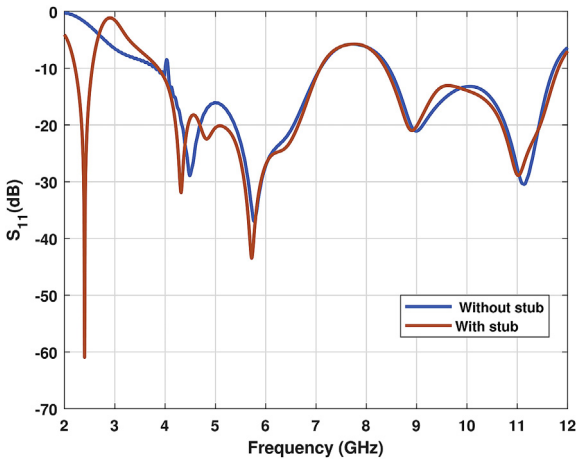

Figure 5. Effect of the stub on the proposed antenna.

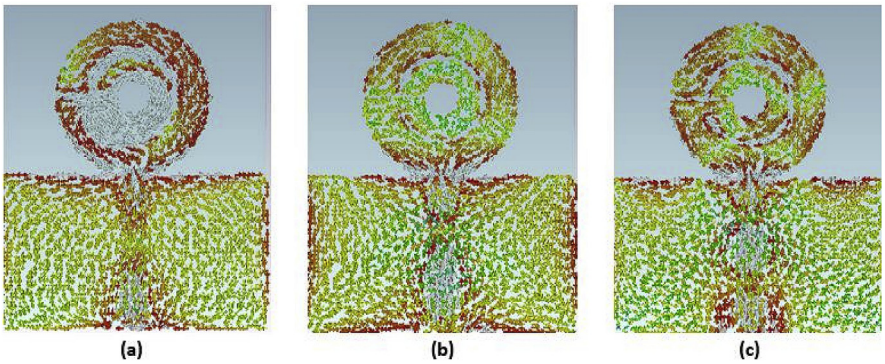

Figure 6. Surface current distribution at (a) 2.45 GHz (b) 6 GHz (c) 9 GHz.

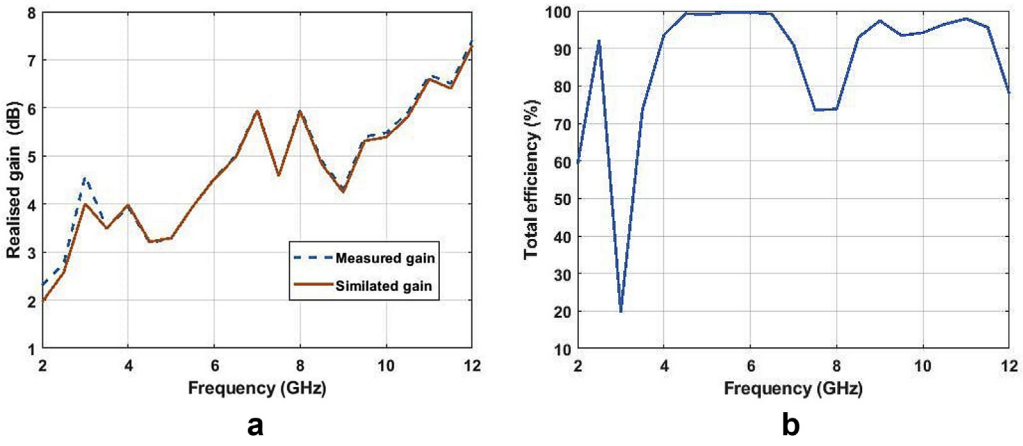

Figure 7. (a) Prototype of the proposed antenna (b) Simulated and measured S_{11} results.

simulated and measured results are shown in Figure 7. We measured the return loss performance and radiation patterns in the anechoic chamber. The experimental set up and the validation of the results have been displayed in Figure 8. We analysed the simulated and measured results of the proposed antenna. It is observed that in most cases, there is good agreement of both simulated and measured results. Figure 7(b) show the results of simulated and measured return loss performance of the antenna. It can be observed that the proposed antenna shows a good impedance matching at the ISM band 2.45 GHz and a satisfactory large bandwidth in the UWB spectrum from 3.4-11.8 GHz, although we

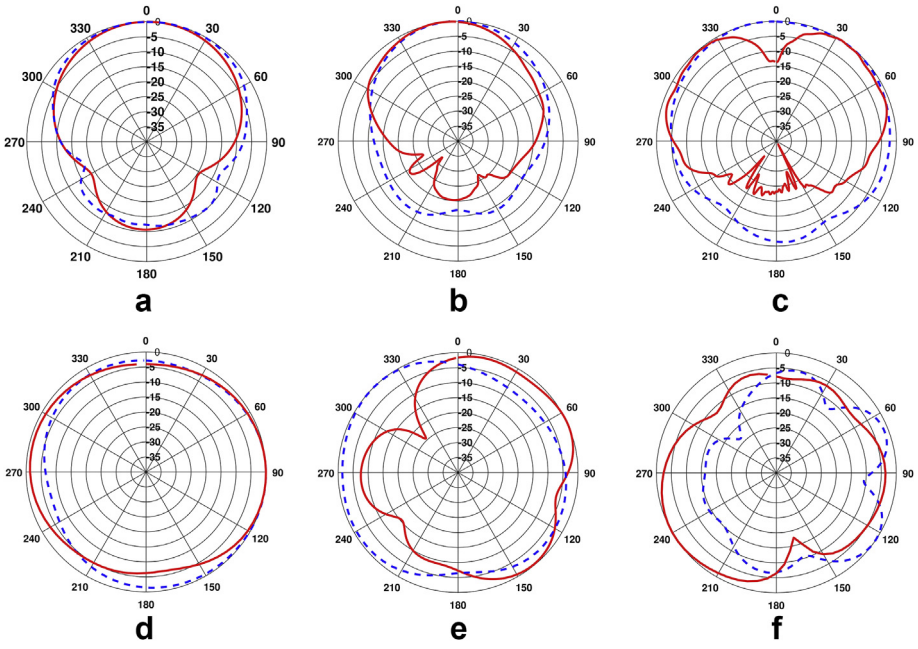

Figure 8. Experimental set up (a) Screenshot of measured S_{11}, (b) radiation pattern measurement in anechoic chamber.

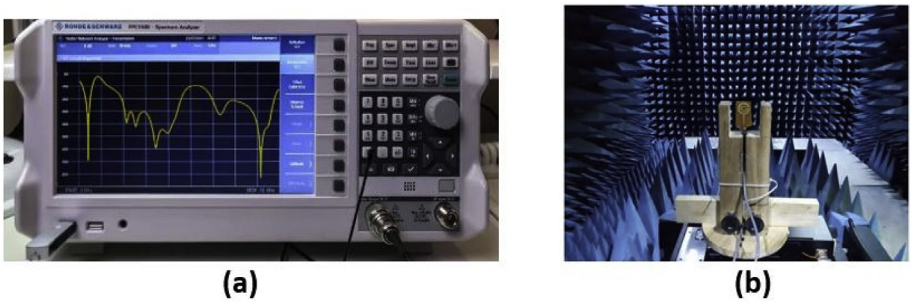

Figure 9. Simulated (dotted line) and measured (solid line) radiation patterns at 4.5 GHz, 6 GHz and 9 GHz. (a–c) azimuthal plane, (d–f) elevation plane.

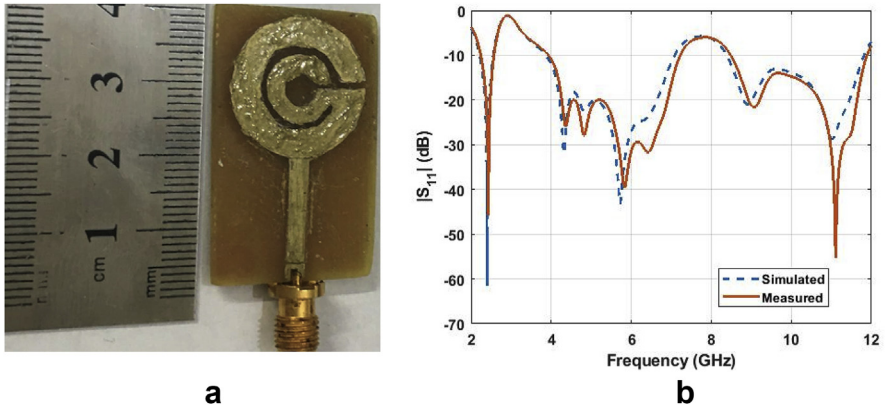

Figure 10. (a) Simulated and measured gain (b) Efficiency of the proposed antenna.

Table 2. Comparison of proposed design and others reported in the literature.

Ref	Antenna Size (mm^2)	${}^{\lambda}g = \frac{\lambda}{\sqrt{\epsilon}}$ (m)	Elec. size $\lambda = c/f_{low}$	Gain(dBi)	Efficiency (%)>	Methodology	-10 dB (GHz)
[34]	21.0 × 28.0	0.042	0.26λ × 0.35λ	5	65	*L−shaped SRR*	*Multibands*
[35]	36.0 × 22.0	0.072	0.24λ × 0.15λ	5	–	*SRR*	*T ripleBand*
[36]	36.0 × 24.0	0.048	0.35λ × 0.24λ	5.2	90	*Compact uniplanar FSS*	2.94–15.26
[37]	19.0 × 23.35	0.048	0.19λ × 0.23λ	3.9	70	*Hexagonal SRR*	3.0–20.0
[38]	64.0 × 64.0	0.074	0.58λ × 0.58λ	11.8	–	*Ellipse patches*	2.7–9.5
[39]	64.0 × 37.4	0.107	0.32λ × 0.19λ	6.8	90	*Half − ellipse patch*	1.5–10.4
[40]	91.1 × 67.6	0.057	0.85λ × 0.63λ	9.2	90	*CPW -fed elliptical monopole*	2.8–20
[41]	77.0 × 35.0	0.113	0.37λ × 0.17λ	6.9	–	*Fractal complimentary slot*	1.44–18.8
Proposed	40.0 × 30.0	0.041	0.45λ × 0.34λ	7	93	*CircularSplit ring resonator*	3.4–7.0 & 8–11.4

acknowledge a slight notch between 7-8 GHz. We also compared the simulated and measured radiation patterns; the result is depicted in Figure 9. It is observed that there is good agreement of both simulated and measured results at the sampled frequencies. The radiation pattern is nearly omnidirectional in the elevation plane. In the azimuthal plane, the pattern is quasi-directional. The peak gain and the efficiency of the antenna are depicted in Figure 10. It is noticed that a reasonable gain performance is obtained and the efficiency is above 93% and better than those reported in the literature [34, 35, 36, 37, 39, 40]. Table 2 shows a comparison between the proposed design and other designs reported. It is observed that the proposed antenna is comparable or better in terms of dimension and band of operations. The proposed structure is designed for dual-band operation at the ISM band (2.4 GHz) and in the ultra-wideband (UWB) spectrum (3.1–10.6 GHz)

4. Conclusion

A novel split ring radiator (SRR) for dual-spectrum has been presented to work in ISM band 2.45 GHz and UWB spectrum simultaneously. The proposed SRR sensitive parameters such as the effects of the aperture (slit), coupling gap, and stub are analyzed for better impedance matching and bandwidth enhancement. The efficiency of the SRR-loaded monopole exceeds 90% at the associated bands. The proposed structure is simple, low-profile and can be integrated on printed circuit board and suitable for short range wireless communications and microwave imaging. The antenna also provides stable radiation patterns as desired for ISM 2.45 GHz band and UWB spectrum.

Declarations

Author contribution statement

Bright Yeboah-Akowuah: Conceived and designed the experiments; Analyzed and interpreted the data; Wrote the paper.

Eric Tutu Tchao: Performed the experiments; Analyzed and interpreted the data.

Masood Ur-Rehman: Conceived and designed the experiments; Analyzed and interpreted the data.

Mohammad Monirujjaman Khan: Analyzed and interpreted the data; Contributed reagents, materials, analysis tools or data; Wrote the paper.

Sarosh Ahmad: Performed the experiments.

Funding statement

This research did not receive any specific grant from funding agencies in the public, commercial, or not-for-profit sectors.

Data availability statement

Data will be made available on request.

Declaration of interests statement

The authors declare no conflict of interest.

Additional information

No additional information is available for this paper.

References

[1] Y. Chen, Y. Jiao, G. Zhao, F. Zhang, Z. Liao, Y. Tian, Dual-band dual-sense circularly polarized slot antenna with a c-shaped grounded strip, IEEE Antenn. Wireless Propag. Lett. 10 (2011) 915–918.
[2] X.Y. Zhang, Z.J. Zhang, W. Duan, Y.F. Cao, Compact high gain dual-band dual-polarized base station antenna, in: 2018 International Symposium on Antennas and Propagation (ISAP), 2018, pp. 1–2.
[3] P. Li, K.M. Luk, K.L. Lau, A dual-feed dual-band l-probe patch antenna, IEEE Trans. Antenn. Propag. 53 (7) (2005) 2321–2323.
[4] T.T. Le, T.Y. Yun, Miniaturization of a dual-band wearable an- tenna for wban applications, IEEE Antenn. Wireless Propag. Lett. 19 (8) (2020) 1452–1456.
[5] C. Zhou, L. Guo, H. Sun, H. Li, M. Li, A wideband dual-polarized dual-mode antenna with simple differential feeding, IEEE Antenn. Wireless Propag. Lett. 19 (10) (2020) 1664–1668.
[6] Z. Yang, S. Xiao, L. Zhu, B. Wang, H. Tu, A circularly polarized implantable antenna for 2.4-ghz ism band biomedical applications, IEEE Antenn. Wireless Propag. Lett. 16 (2017) 2554–2557.
[7] D. Wu, Y. Zang, H. Luyen, M. Li, N. Behdad, A compact, low-profile simultaneous transmit and receive antenna with monopole- like radiation characteristics, IEEE Antenn. Wireless Propag. Lett. 18 (4) (2019) 611–615.
[8] X. Yang, H. Wong, J. Xiang, Polarization reconfigurable planar inverted-f antenna for implantable telemetry applications, IEEE Access 7 (2019) 141900–141909.
[9] Federal Communications Commission Revision of Part 15 of the Com- mission's Rules Regarding Ultra-wideband Transmission Systems 48 (2002). FCC, Washington, DC, First Report and Order FCC, 02.
[10] IEEE standard for information technology [Online] Available, Dec. 2020, https://standards.ieee.org/standard/802 11b-1999.html.
[11] Y. Liu, P. Liu, Z. Meng, L. Wang, Y. Li, A planar printed nona- band loop-monopole reconfigurable antenna for mobile handsets, IEEE Antenn. Wireless Propag. Lett. 17 (8) (2018) 1575–1579.
[12] M.S. Ellis, A. Ahmed, J.J. Kponyo, J. Nourinia, C. Ghobadi, B. Mohammadi, Unidirectional planar monopole antenna using a quasi- radiator, IEEE Antenn. Wireless Propag. Lett. 18 (1) (2019) 157–161.
[13] L.Y. Nie, X.Q. Lin, Z.Q. Yang, J. Zhang, B. Wang, Structure- shared planar uwb mimo antenna with high isolation for mobile plat- form, IEEE Trans. Antenn. Propag. 67 (4) (2019) 2735–2738.
[14] B. Yeboah-Akowuah, P. Kosmas, Y. Chen, A q-slot monopole for uwb body-centric wireless communications, IEEE Trans. Antenn. Propag. 65 (10) (2017) 5069–5075.
[15] H. Nawaz, X. Liang, M.S. Sadiq, J. Geng, W. Zhu, R. Jin, Ruggedi- zed planar monopole antenna with a null-filled shaped beam, IEEE Antenn. Wireless Propag. Lett. 17 (5) (2018) 933–936.
[16] A. Chen, M. Sun, Z. Zhang, X. Fu, Planar monopole antenna with a parasitic shorted strip for multistandard handheld terminals, IEEE Access 8 (2020) 51647–51652.
[17] M. Midya, S. Bhattacharjee, M. Mitra, Broadband circularly polarized planar monopole antenna with g-shaped parasitic strip, IEEE Antenn. Wireless Propag. Lett. 18 (4) (2019) 581–585.
[18] M.S. Ellis, A. Ahmed, J.J. Kponyo, J. Nourinia, C. Ghobadi, B. Mohammadi, Unidirectional planar monopole antenna using a quasi- radiator, IEEE Antenn. Wireless Propag. Lett. 18 (1) (2019) 157–161.
[19] X. Wang, Y. Wu, W. Wang, A.A. Kishk, A simple multi- broadband planar antenna for lte/gsm/umts and wlan/wimax mobile handset applications, IEEE Access 6 (2018) 74453–74461.
[20] J. Chen, S. Cao, X. Zhang, Spps-shared dual-band antenna with large frequency ratio, IEEE Access 8 (2020) 29132–29139.
[21] N. Agrawall, G. Kumar, K. Ray, Wide-band planar monopole antennas, IEEE Trans. Antenn. Propag. 46 (2) (1998) 294–295.
[22] A. Deshmukh, G. Kumar, Formulation of resonant frequency for compact microstrip antennas, in: 2006 IEEE Antennas and Propagation Society International Symposium, 2006, pp. 1981–1984.
[23] A.A. Deshmukh, K.P. Ray, Analysis of shorted-plate compact and broadband microstrip antenna, IEEE Antenn. Propag. Mag. 55 (6) (2013) 100–113.
[24] A. Holub, M. Polivka, "A novel microstrip patch antenna miniatur- ization technique: a meanderly folded shorted-patch antenna, in: 2008 14th Conference on Microwave Techniques, 2008, pp. 1–4.
[25] R. Hussain, M.U. Khan, M.S. Sharawi, Design and analysis of a miniaturized meandered slot-line-based quad-band frequency agile mimo antenna, IEEE Trans. Antenn. Propag. 68 (3) (2020) 2410–2415.
[26] L. Guo, M. Min, W. Che, W. Yang, A novel miniaturized planar ultra-wideband antenna, IEEE Access 7 (2019) 2769–2773.
[27] M. Shokri, H. Shirzad, S. Movagharnia, B. Virdee, Z. Amiri, S. Asi- aban, Planar monopole antenna with dual interference suppression functionality, IEEE Antenn. Wireless Propag. Lett. 12 (2013) 1554–1557.
[28] J.Y. Siddiqui, C. Saha, Y.M.M. Antar, Compact srr loaded uwb circular monopole antenna with frequency notch characteristics, IEEE Trans. Antenn. Propag. 62 (8) (2014) 4015–4020.
[29] F.J. Herraiz-Martinez, L.E. Garcia-Munoz, D. Gonzalez-Ovejero, V. Gonzalez-Posadas, D. Segovia-Vargas, Dual-frequency printed dipole loaded with split ring resonators, IEEE Antenn. Wireless Propag. Lett. 8 (2009) 137–140.
[30] F.J. Herraiz-Martinez, D. Segovia-Vargas, L.E. Garcia-Munoz, V. Gonzalez-Posadas, Dual-frequency printed dipole loaded with meta- material particles, in: 2008 IEEE Antennas and Propagation Society International Symposium, 2008, pp. 1–4.
[31] M. Li, X. Chen, A. Zhang, W. Fan, A.A. Kishk, Split-ring resonator-loaded baffles for decoupling of dual-polarized base station array, IEEE Antenn. Wireless Propag. Lett. 19 (10) (2020) 1828–1832.
[32] M. Agarwal, J.K. Dhanoa, M.K. Khandelwal, Two-port hexagon shaped mimo microstrip antenna for uwb applications integrated with double stop bands for wimax and wlan, AEU - Int. J. Electr. Commun. 138 (2021) 153885.
[33] M. Aminu-Baba, M.K.A. Rahim, F. Zubir, A.Y. Iliyasu, K.I. Jahun, M.F.M. Yusoff, M. Gajibo, A. Pramudita, I.K.C. Lin, A compact triband miniaturized mimo antenna for wlan applications, AEU - Int. J. Electr. Commun. 136 (2021) 153767.
[34] I.J. Rajmohan, M.I. Hussein, A compact multiband planar antenna using modified l-shape resonator slots, Heliyon 6 (10) (2020), e05288.
[35] K. Patchala, Y. Raja Rao, A. Prasad, Triple band notch compact mimo antenna with defected ground structure and split ring resonator for wideband applications, Heliyon 6 (1) (2020), e03078.
[36] S. Kundu, "High gain compact ultra-wideband "antenna-frequency selec- tive surface" and its performance evaluation in proximity of soil surface, Microw. Opt. Technol. Lett. 63 (3) (2021) 869–875.
[37] M.T. Islam, F.B. Ashraf, T. Alam, N. Misran, K.B. Mat, A compact ultrawideband antenna based on hexagonal split-ring resonator for ph sensor application, Sensors (Basel, Switzerland) 18 (09 2018) 2959.
[38] J.-Y. Li, R. Xu, X. Zhang, S.-G. Zhou, G.-W. Yang, A wideband high-gain cavity-backed low-profile dipole antenna, IEEE Trans. Antenn. Propag. 64 (12) (2016) 5465–5469.
[39] Z. Li, C. Yin, X. Zhu, Compact uwb mimo vivaldi antenna with dual band-notched characteristics, IEEE Access 7 (2019) 38696–38701.
[40] J.F. Liu, W. Tang, M. Wang, H.C. Zhang, H.F. Ma, X. Fu, T.J. Cui, A dual-mode uwb antenna for pattern diversity application, IEEE Trans. Antenn. Propag. 68 (4) (2020) 3219–3224.
[41] K.-R. Chen, C.-Y.-D. Sim, J.-S. Row, A compact monopole antenna for super wideband applications, IEEE Antenn. Wireless Propag. Lett. 10 (2011) 488–491.